6348 *Macromolecules* **2010**, *43*, 6348–6352
DOI: 10.1021/ma100997g

Macromolecules
ARTICLE

Synthesis and Characterization of Thiophene-Containing Naphthalene Diimide n-Type Copolymers for OFET Applications

Matthew M. Durban,[†] Peter D. Kazarinoff,[‡] and Christine K. Luscombe*[,‡]

[†]*Department of Chemistry, University of Washington, Seattle, Washington 98195-1750, and* [‡]*Department of Material Science and Engineering, University of Washington, Seattle, Washington 98195-2120*

Received May 4, 2010; Revised Manuscript Received June 25, 2010

ABSTRACT: Naphthalene diimide (NDI) copolymers are attractive n-type materials for use in organic electronic devices. Four highly soluble NDI polymers are presented—each differing only in the thiophene content comprising the material. Electron mobilities as high as 0.076 $cm^2\ V^{-1}\ s^{-1}$ for the novel material **PNDI-3Th** are reported. Polymer crystallinity and general macromolecular order are shown to effectively improve by increasing the number of thiophene units within the polymer backbone. The structure−property relationship of NDI−thiophene copolymers is presented and discussed as it pertains to organic field effect transistor (OFET) performance.

Introduction

Growth in the field of organic electronic materials and devices has led toward the development of new solution-processable high-performance n-type polymers and small molecules with the hope of generating efficient, low-cost, and flexible organic electronic devices.[1−6] Semiconducting materials with strong electron-withdrawing groups comprising the structure have been used to develop n-type functionality within solution processable polymers based on naphthalene[7,8] and perylene diimide[9−12] as well as the ladder-polymer BBL[13] and others.[14,15] Naphthalene diimide (NDI) polymers in particular have begun to attract a great deal of attention with the recent report of a soluble naphthalene diimide−bithienyl copolymer capable of being used in printable electronics applications and achieving organic field-effect transistor (OFET) electron mobilities reported up to 0.85 $cm^2\ V^{-1}\ s^{-1}$ using top-gate bottom-contact device architectures with polymeric dielectrics.[7] An NDI-functionalized thiophene copolymer yielding high-performing ambipolar OFET devices was also recently reported in the literature.[16] These developments with regard to n-type semiconductor performance provide further support and incentive toward the fabrication of complementary circuits possessing enhanced performance and device operation.[17,18]

Further development into this chemical architecture is examined and presented in this report through the synthesis and characterization of a series of soluble high-performance naphthalene diimide−core donor−acceptor based polymers (**PNDI-0Th**, **PNDI-1Th**, **PNDI-2Th**, and **PNDI-3Th** shown in Scheme 1) possessing n-type character. Electron mobilities as high as 0.076 $cm^2\ V^{-1}\ s^{-1}$ for the material **PNDI-3Th** were achieved using top-contact bottom-gate organic field-effect transistor (OFET) architectures with SiO_2 as the dielectric. By comparison, comparable electron mobilities as high as ~0.06 $cm^2\ V^{-1}\ s^{-1}$ were reported for **PNDI-2Th** by Facchetti et al. using the same OFET architectures as are presented in this report.[19] X-ray diffraction (XRD) results helped to confirm a progressive increase in thin-film crystallinity and subsequent decrease in amorphous character with the inclusion of a greater number of thiophene subunits within the backbone of the polymer.

*Corresponding author. E-mail: luscombe@u.washington.edu.

Scheme 1. NDI Polymer Synthesis

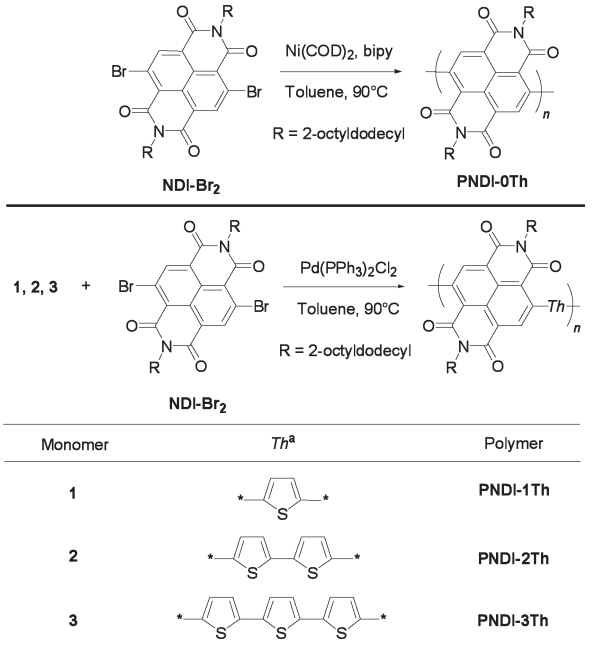

[a] Asterisks indicated stannyl moieties: monomer 1,2 = tributyltin, monomer 3 = trimethyltin.

Experimental Section

Instrumentation and Materials. ^1H NMR spectra were obtained using a Bruker AV-300 spectrometer. Polymer molecular weights were obtained using a Waters-1515 gel permeation chromatograph (GPC) coupled with UV and RI detectors. Polystyrene GPC standards in THF were used as a reference. Cyclic voltammetry for all polymers was obtained under nitrogen using a BAS CV-50W voltammetric analyzer with 0.1 M tetra-*n*-butylammonium hexafluorophosphate in anhydrous acetonitrile as supporting electrolyte. A platinum wire working and counter electrode as well as an $Ag/AgNO_3$ reference electrode was used, and ferrocene (Fc/Fc^+) was designated as an internal standard for all measurements. The scan rate was 50 mV s^{-1}. The reference energy level used for ferrocene as

 Published on Web 07/13/2010 © 2010 American Chemical Society

Table 1. Polymer Properties and Yields

	yield (%)	M_n [PDI][a] (kDa)	soln λ_{max}[b] abs (nm)	film λ_{max}[c] abs (nm)	E_g^{opt}[d] (eV)	$E_{1/2red}$[e] (V)	LUMO[f] (eV)	HOMO[g] (eV)
PNDI-0Th	70	71.1 [2.9]	409	426	2.74	−0.93	−3.76	−6.50
PNDI-1Th	87	14.5 [2.5]	548	623	1.77	−0.84	−3.85	−5.62
PNDI-2Th	95	46.9 [2.1]	672	696	1.50	−0.90	−3.79	−5.30
PNDI-3Th	97	153 [2.2]	701	742	1.37	−0.94	−3.76	−5.13
NDI-Br_2			406	411	2.90			

[a] Number-average molecular weight and polydispersity (SEC vs polystyrene standards in THF). [b] Solution absorption spectra ($\sim 5 \times 10^{-6}$ M $CHCl_3$). [c] Thin film absorption spectra from spin-cast $CHCl_3$ solutions. [d] Optical energy gap estimated from the absorption-edge or onset of organic thin films. [e] CV measurements of thin films vs Fc/Fc^+. [f] Estimated from LUMO = −(normalized Fc/Fc^+) − $E_{1/2red}$. [g] Estimated from HOMO = LUMO − E_g^{opt}.

compared to vacuum was 4.8 eV. A HP4145B semiconductor parameter analyzer controlled by locally written LabView codes through a GPIB interface was used for OFET device characterization. All device fabrication and electrical characterization were performed in a nitrogen atmosphere. Samples for UV/vis and X-ray diffraction analysis were cleaned prior to use. Absorption spectra were obtained using a Perkin-Elmer spectrophotometer (Lambda 9 UV/vis/NIR). X-ray diffraction patterns were obtained on a Bruker AXS D8 Focus diffractometer using an accelerating voltage of 40 kV and a Cu Kα source. AFM images were taken on a Veeco multimode AFM in tapping mode with a Nanoscope IIIa controller and etched silicon tips having a typical resonant frequency of 300−350 kHz. All reagents used for synthesis were obtained from Sigma-Aldrich and were used as-is without further purification with the exception of the two catalysts: $Ni(COD)_2$ and $Pd(PPh_3)_2Cl_2$, which were obtained from Strem Chemicals.

Synthetic Procedures. The monomers used to synthesize the four NDI polymers were synthesized using standard literature procedures—specifically, NDI-Br_2[7,8,19,20] and the stannylated thiophenes **1**, **2**, and **3**.[8,21]

*Synthesis of **PNDI-0Th***. To an air-free Schlenk flask, $Ni(COD)_2$ (0.179 g, 0.65 mmol), 2,2′-bipyridine (0.064 g, 0.41 mmol), and COD (0.07 g, 0.65 mmol) were added within a dry glovebox and dissolved with toluene (1.5 mL) and DMF (0.35 mL). The capped and sealed vessel was heated to 80 °C for 30 min prior to injecting a solution of NDI-Br_2 (0.2 g, 0.28 mmol) in toluene (1.5 mL). The reaction was heated at 80 °C for 6 days. The reaction was cooled to ambient and quenched with 2 N HCl (2 mL) and stirred for 15 min. Chloroform was added (25 mL) and extracted. The organic layer was washed twice with 2 N HCl (20 mL). The aqueous layers were combined and extracted twice with chloroform. The organics were combined and stirred with a saturated Na_4EDTA solution (10 mL) for 12 h. The organics were washed with water, dried over $MgSO_4$, and filtered over a pad of silica. The solution was concentrated and precipitated to methanol. The precipitated polymer was subjected to a Soxhlet extraction with acetone to remove low-molecular-weight polymer fragments. The polymer was redissolved in chloroform and precipitated into methanol to yield a fibrous yellow solid (70%). ^1H (300 MHz, $CDCl_3$): 8.65 (br s, 2H), 3.98 (br, 4H), 1.91 (m, 2H), 1.24 (m, 64H), 0.86 (m, 12H).

*General Synthesis for **PNDI-n-Th***. To an air-free Schlenk flask, $Pd(PPh_3)_2Cl_2$ (0.005 mmol), NDI-Br_2 (0.10 mmol), and **1**,[8] **2**,[8] or **3**[21] (0.10 mmol) were added within a dry glovebox and dissolved with toluene (5 mL). The capped and sealed vessel was heated at 90 °C for 4 days prior to injecting bromobenzene (0.2 mL) and stirring for 12 h. The reaction was cooled to ambient and KCl (1 g) in water (2 mL) was injected and stirred for 2 h. The solution was extracted with chloroform (2 × 60 mL). The combined organics were washed with water (2 × 50 mL) and dried over Na_2SO_4. The solution was concentrated by vacuum and precipitated into methanol. The precipitated polymer was subjected to a Soxhlet extraction with acetone for 48 h to remove low-molecular-weight polymer fragments. The polymer was redissolved in chloroform, precipitated into methanol, and dried under reduced pressure. See Table 1 for further polymer data. **PNDI-1Th**: Dark blue solid (87%). ^1H (300 MHz, $CDCl_3$): 8.97 (br s, 2H), 7.45 (br, 2H), 4.14 (br, 4H), 2.02 (m, 2H), 1.10−1.45 (m, 64H), 0.83 (m, 12H). **PNDI-2Th**: Dark blue solid (95%). ^1H (300 MHz, $CDCl_3$): 8.80 (br s, 2H), 7.33 (br, 4H), 4.11 (br, 4H), 2.04 (m, 2H), 1.07−1.54 (m, 64H), 0.86 (m, 12H). **PNDI-3Th**: Dark green solid (97%). ^1H (300 MHz, $CDCl_3$): 8.80 (br s, 2H), 7.32 (br, 6H), 4.10 (br, 4H), 1.97 (m, 2H), 1.08−1.60 (m, 64H), 0.87 (m, 12H).

OFET Device Fabrication. Organic field-effect transistors were fabricated as typical top-contact bottom-gate devices on silicon substrates. Heavily doped p-type silicon ⟨100⟩ substrates from Montco Silicon Technologies Inc. with a 500 ± 5 nm thermal oxide layer acted as a common gate with a dielectric layer as well as the substrate. After cleaning the substrates by sequential ultrasonication in acetone, methanol, and isopropyl alcohol for 10 min, the substrates were treated by air plasma prior to forming a self-assembled monolayer of octadecyltrichlorosilane (OTS) via vapor deposition. The substrates were then washed with chloroform and isopropyl alcohol to remove physisorbed silane agents. Polymer thin films were deposited from a 5 mg/mL chloroform:*o*-DCB solution (98:2) by spin-coating (1000 rpm for 60 s). The devices were thermally annealed with varying temperature lengths to optimize device performance. The **PNDI-0Th**, **PNDI-1Th**, and **PNDI-3Th** polymers were all annealed at 150 °C; the **PNDI-2Th** polymer was annealed at 110 °C. Interdigitated source and drain electrodes (W = 9000 μm, L = 90 μm) made of gold (50 nm thick) were deposited on top of the polymer active layer by thermoevaporation at 1.0 Å/s through a shadow mask from a resistively heated Mo boat under high vacuum (5.0×10^{-7} Torr).

Results and Discussion

The highly electron-deficient napthelene diimide acceptor unit with branched-alkane, octyldodecyl-, solubilizing groups was copolymerized with stannylated thiophene, bithiophene, and terthiophene donor units using Stille conditions and $Pd(PPh_3)_2Cl_2$ as catalyst. The homopolymerization was performed via Yamamoto coupling conditions using $Ni(COD)_2$/bipy as catalyst. The copolymer **PNDI-2Th** has been reported[7,19] in the literature, and an analogue of **PNDI-1Th** has been synthesized previously.[8] An NDI homopolymer (Scheme 1) was synthesized to analyze the elongation of the conjugation length relative to the NDI monomer on its own and as the number of thiophenes integrated within the backbone of the polymer is increased.

The molecular weights of all the polymers synthesized were determined using size-exclusion chromatography relative to polystyrene standards in THF and are listed in Table 1. The polymer molecular weights were recognized as being overestimations of the actual polymer mass due to NDIs possessing rigid-rod-like character.[22] Additionally, the polymer **PNDI-3Th** with an M_n = 153 kDa may have generated aggregates due to being much less soluble than the polymers with fewer thiophene units which would further yield a higher than expected polymer molecular weight as a result of a faster elution time with size exclusion chromatography (GPC).

Optical absorption spectra (Figure 1) were taken for all four polymer films spin-coated from $CHCl_3$ onto glass revealing a progressive red-shifting of the absorption band (with increasing thiophene units in the polymer chain) from λ_{max} = 426 nm for

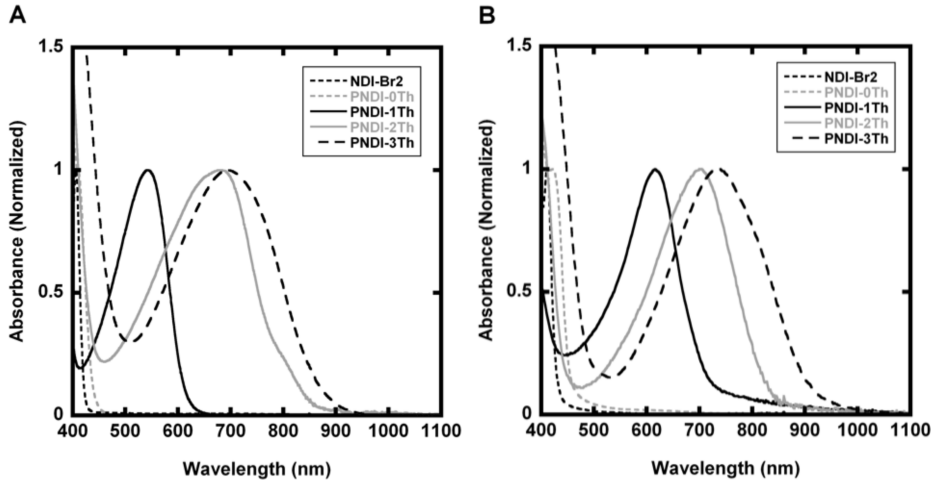

Figure 1. (A) Solution UV/vis absorption spectra ($\sim 5 \times 10^{-6}$ M $CHCl_3$) and (B) thin-film UV/vis absorption spectra.

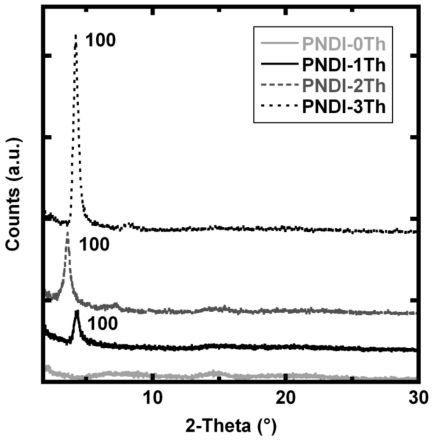

Figure 2. X-ray diffraction patterns of NDI polymers.

PNDI-0Th to $\lambda_{max} = 742$ nm for **PNDI-3Th**. This shift reveals an effective π-conjugation length elongation likely due to the improved rigidity and planarization of the polymer as a result of the strong $\pi-\pi$ interactions of the thiophene units.[23,24] This notion was further confirmed with X-ray diffraction (XRD) by analyzing the relative crystallinities of the four polymers in the solid state; the data are presented in Figure 2.[25] The XRD spectrum for **PNDI-0Th** shows no visible peaks, while the spectra for **PNDI-1Th** and **PNDI-3Th** both show the 100 peak at $2\theta = \sim 4.2°$ and **PNDI-2Th** shows its 100 peak at $2\theta = \sim 3.6°$ (Figure 2). These values correspond to an interchain lamellar *d*-spacing of 21.0 Å for **PNDI-1Th** and **PNDI-3Th** and 24.5 Å for **PNDI-2Th**. While all three PNDI copolymers appear to be at least somewhat amorphous, **PNDI-3Th** was observed to exhibit the greatest relative crystallinity of the PNDI series (as governed by the 100 peak intensities), followed by **PNDI-2Th** and finally **PNDI-1Th**. The lack of diffraction peaks in the **PNDI-0Th** spectrum indicates that the homopolymer has very little, if any, long-range order in the solid state. This is further supported by the lack of a significant shift between the solution and solid state UV/vis spectra of **PNDI-0Th**.

AFM images were taken from OTS-treated and annealed films of the four polymers to verify the presence of contrasting morphological or crystalline features which were detected with XRD. As seen in Figure 3, **PNDI-0Th** and **PNDI-1Th** were observed to show little to no self-organization within the size scales obtainable using AFM imaging methods. **PNDI-2Th** displayed rodlike features at nanometer scales which assembled into featherlike patterns. Films of **PNDI-3Th** also showed rod or

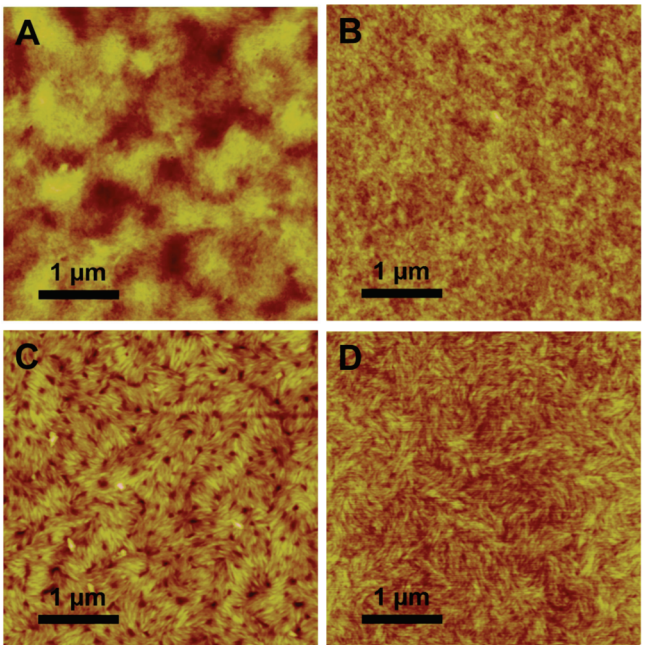

Figure 3. Tapping mode AFM height images of PNDI thin films on OTS-treated Si/SiO_2 wafers processed and annealed under the same conditions as OFETs: (A) **PNDI-0Th**, (B) **PNDI-1Th**, (C) **PNDI-2Th**, and (D) **PNDI-3Th**.

beltlike structures at smaller length scales than **PNDI-2Th** films and also assembled in forming featherlike patterns. These images in conjunction with data obtained by XRD suggest that thin films generated from **PNDI-2Th** and **PNDI-3Th** do in fact possess greater crystallinity compared to films from **PNDI-0Th** and **PNDI-1Th**. We conclude that this observed increase in relative crystallinity (with increasing thiophene content) likely contributed to **PNDI-3Th** possessing a higher charge carrier mobility than **PNDI-0Th**.

The absorption spectrum of **NDI-Br$_2$** was also obtained to observe and compare any potential change in the extent of conjugation for **PNDI-0Th**. It was noted from the absorption spectrum that the conjugation length of the homopolymer does not appear to increase likely due to poor $\pi-\pi$ packing of the material as a result of the bulky octyldodecyl solubilizing chain interference generating twists to the polymer backbone.

The LUMO energy levels were calculated from the onset of the first polymer reduction peak using cyclic voltammetry. Cyclic voltammetry was carried out in a standard three-electrode

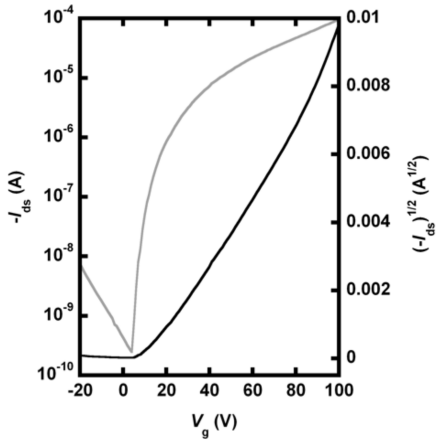

Figure 4. Transfer curve of **PNDI-3Th** at a constant source-drain voltage of +100 V plotted with the square root of current as a function of gate voltage.

electrochemical cell employed with a platinum working electrode and a $Ag/AgNO_3$ reference electrode while using ferrocene as an internal standard. The cyclic voltammograms are shown in the Supporting Information. The energy level referenced for ferrocene compared to vacuum was 4.8 eV.[26] The LUMO values for all four polymers were found to be approximated to ~−3.8 eV due to the intrinsic properties of NDI.[7,19,27] The HOMO values were calculated using the optical band gap (E_g^{opt}) from the calculated LUMO. The compiled data are presented in Table 1. No oxidation waves were observed for any of the four NDI polymers. The electronic properties of the NDI constituting the LUMO of the polymer and the thienyl unit affecting the HOMO and E_g^{opt} of the material were further confirmed by reports stating similar values for related materials.[8,28,29] It is noted that specific tuning of the band gap and HOMO of NDI-based polymers can be achieved by altering the thienyl content of the bulk structure which is similarly achieved in polyfluorenes.[30]

OFET devices were fabricated from the four polymers in the typical top-contact bottom-gate geometry on octydecyltrichlorosilane (OTS)-treated doped-Si/SiO_2 wafers. The active layer of the devices was spin-cast from a 98:2 v/v solution of $CHCl_3$ and *o*-DCB. The polymers produced visually smooth and continuous films. All fabrication and testing was performed in an inert nitrogen atmosphere.

All four polymers showed n-type behavior at positive gate-source biases (V_g = +100 V). The polymers did not display ambipolar or p-type response, with low current flow and on/off ratios below 10 when a negative gate-source bias was applied (V_g = −100 V). The saturated charge carrier mobility of the four polymers was calculated using the saturation current equation: $I_{ds} = (\mu WC_0/2L)(V_g - V_t)^2$.[31]

A linear fit was applied in the saturation region of the $I_{ds}^{1/2}$ vs V_G curve of each of the polymers in order to calculate the mobility. An electron mobility (μ_e) as high as 0.076 $cm^2\ V^{-1}\ s^{-1}$ was measured for OFETs produced from **PNDI-3Th** (Figure 4). (Transfer curves for all polymers are included in the Supporting Information.) As shown in Table 2, **PNDI-3Th** was found to possess the highest charge carrier mobility which was closely followed by **PNDI-2Th** (3.9×10^{-2} $cm^2\ V^{-1}\ s^{-1}$). This value is comparable to a prior report in which the mobility for **PNDI-2Th** was measured to be ~6.0×10^{-2} $cm^2\ V^{-1}\ s^{-1}$ for devices using similar architectures.[19] **PNDI-1Th** and **PNDI-0Th** had significantly lower electron mobilites of 3.1×10^{-3} and 6×10^{-4} $cm^2\ V^{-1}\ s^{-1}$, respectively. The on/off ratios followed a similar trend. **PNDI-2Th** and **PNDI-3Th** displayed the largest on/off ratios (10^5) whereas **PNDI-0Th** yielded the lowest (10^3). The larger on/off ratios of **PNDI-2Th** and **PNDI-3Th** are mostly due to a larger on-current, where as the off-current value for all four polymers was within the same order of magnitude.

Table 2. Electrical Characterization of Thiophene Copolymers

	T_a[a] (°C/h)	μ_e[b] ($cm^2\ V^{-1}\ s^{-1}$)	$I_{on/off}$	V_t (V)
PNDI-0Th	180/2	6×10^{-4} ($\pm 2 \times 10^{-4}$)	10^3	40
PNDI-1Th	150/0.16	3.1×10^{-3} ($\pm 3 \times 10^{-4}$)	10^3	20
PNDI-2Th	110/4	3.9×10^{-2} ($\pm 3 \times 10^{-3}$)	10^5	10
PNDI-3Th	150/0.16	7.6×10^{-2} ($\pm 4 \times 10^{-3}$)	10^5	7

[a] Annealing temperature and time annealed. [b] Average value of 3−4 devices with standard deviation. Calculated from the $I_{ds}^{1/2}$ vs V_g plot using the equation $I_{ds} = (\mu WC_0/2L)(V_g - V_t)^2$.

The threshold voltage (V_t) was calculated as the *x*-intersect of this linear fit line. Following a similar performance trend, **PNDI-3Th** had the lowest threshold voltage while **PNDI-0Th** had the highest. The electrical characterization results are summarized in Table 2. From this data it is clear that within the series of four polymers presented within this report, increasing the thiophene content of PNDIs improves the electron transport properties of the polymer.

Conclusion

We have demonstrated the synthesis and performance of a series of polymers with high electron mobilities. Electron mobilities as high as 0.076 $cm^2\ V^{-1}\ s^{-1}$ were achieved for TFTs from **PNDI-3Th**. XRD and AFM results suggest increasing the thiophene content of PNDIs effectively increases polymer crystallinity and order to a degree which will lead to improved performance. By employing alternative OFET device architectures such as top-gate bottom-contact and the use of various dielectrics and printing fabrication techniques, the measurable performance of **PNDI-3Th** should be able to exceed that of **PNDI-2Th** (0.85 $cm^2\ V^{-1}\ s^{-1}$) which was reported by Facchetti et al.[7] The high electron mobility, energy levels, and good absorption spectrum of **PNDI-2Th** and **PNDI-3Th** suggest the possibility of yielding other moderately high-performance electronic devices with organic p-type semiconducting materials such as poly(3-hexylthiophene). Research into the performance of devices such as organic photovoltaic (OPV) devices and alternative OFET device conditions and architectures is the subject of future investigation.

Acknowledgment. The authors acknowledge the NSF (CAREER Award DMR 0747489) and Teijin Ltd. for financial assistance and Patrick Shamberger and Fumio Ohuchi for help with the XRD analysis.

Supporting Information Available: Figures showing cyclic voltammetry reduction curves and OFET transfer curves for **PNDI-0Th**, **PNDI-1Th**, and **PNDI-2Th**. This material is available free of charge via the Internet at http://pubs.acs.org.

References and Notes

(1) Liu, S.; Wang, W. M.; Briseno, A. L.; Mannsfeld, S. C. B.; Bao, Z. *Adv. Mater.* **2009**, *21*, 1217.
(2) Allard, S.; Forster, M.; Souharce, B.; Thiem, H.; Scherf, U. *Angew. Chem., Int. Ed.* **2008**, *47*, 4070.
(3) Mas-Torrent, M.; Rovira, C. *Chem. Soc. Rev.* **2008**, *37*, 827.
(4) Cornil, J.; Bredas, J.-L.; Zaumseil, J.; Sirringhaus, H. *Adv. Mater.* **2007**, *19*, 1791.
(5) Murphy, A. R.; Fréchet, J. M. J. *Chem. Rev.* **2007**, *107*, 1066.
(6) Locklin, J.; Roberts, M.; Mannsfeld, S.; Bao, Z. *Polym. Rev.* **2006**, *46*, 79.
(7) Yan, H.; Chen, Z.; Zheng, Y.; Newman, C.; Quinn, J. R.; Dötz, F.; Kastler, M.; Facchetti, A. *Nature* **2009**, *457*, 679.
(8) Guo, X.; Watson, M. D. *Org. Lett.* **2008**, *10*, 5333.
(9) Huttner, S.; Sommer, M.; Thelakkat, M. *Appl. Phys. Lett.* **2008**, *92*, 093302.

(10) See, K. C.; Landis, C.; Sarjeant, A.; Katz, H. E. *Chem. Mater.* **2008**, *20*, 3609.
(11) Jones, B. A.; Facchetti, A.; Wasielewski, M. R.; Marks, T. J. *J. Am. Chem. Soc.* **2007**, *129*, 15259.
(12) Ling, M. M.; Erk, P.; Gomez, M.; Koenemann, M.; Locklin, J.; Bao, Z. *Adv. Mater.* **2007**, *19*, 1123.
(13) Briseno, A.; Mannsfeld, S. C. B.; Shamberger, P. J.; Ohuchi, F. S.; Bao, Z.; Jenekhe, S. A.; Xia, Y. *Chem. Mater.* **2008**, *20*, 4712.
(14) Letizia, J. *J. Am. Chem. Soc.* **2008**, *130*, 9679.
(15) Zhan, X.; Tan, Z.; Domercq, B.; An, Z.; Zhang, X.; Barlow, S.; Li, Y.; Zhu, D.; Kippelen, B.; Marder, S. R. *J. Am. Chem. Soc.* **2007**, *129*, 7246.
(16) Kim, F. S.; Guo, X.; Watson, M. D.; Jenekhe, S. A. *Adv. Mater.* **2010**, *22*, 478.
(17) Crone, B.; Dodabalapur, A.; Lin, Y.-Y.; Filas, R. W.; Bao, Z.; LaDuca, A.; Sarpeshkar, R.; Katz, H. E.; Li, W. *Nature* **2000**, *403*, 521.
(18) Klauk, H.; Zschieschang, U.; Pflaum, J.; Halik, M. *Nature* **2007**, *445*, 745.
(19) Chen, Z.; Zheng, Y.; Yan, H.; Facchetti, A. *J. Am. Chem. Soc.* **2009**, *131*, 8.
(20) Koeckelberghs, G.; De Cremer, L.; Vanormelingen, W.; Dehaen, W.; Verbiest, T.; Persoons, A.; Samyn, C. *Tetrahedron* **2005**, *61*, 687.
(21) Seitz, D. E.; Lee, S. H.; Hanson, R. N.; Bottaro, J. C. *Synth. Commun.* **1983**, *13*, 121.
(22) Avila-Ortega, A.; Vazquez-Torres, H. *J. Polym. Sci., Part A1* **2007**, *45*, 1993.
(23) Brisset, H.; Thobie-Gautier, C.; Jubault, M.; Gorgues, A.; Roncali, J. J. *Chem. Commun.* **1994**, *1*, 1765.
(24) Brisset, H.; Le Moustarder, S.; Blanchard, P.; Illien, B.; Riou, A.; Orduna, J.; Garin, J.; Roncali, J. J. *Mater. Chem.* **1997**, *7*, 2027.
(25) Murthy, N. S.; Minor, H. *Polymer.* **1990**, *31*, 996.
(26) Li, Y. F.; Cao, Y.; Gao, J.; Wang, D. L.; Yu, G.; Heeger, A. J. *Synth. Met.* **1999**, *99*, 243.
(27) Singh, T. B.; Erten, S.; Guenes, S.; Zafer, C.; Turkmen, G.; Kuban, B.; Teoman, Y.; Sariciftci, N. S.; Icli, S. *Org. Electron.* **2006**, *7*, 480.
(28) Thompson, B. C.; Kim, Y. G.; McCarley, T. D.; Reynolds, J. R. *J. Am. Chem. Soc.* **2006**, *128*, 12714.
(29) Blouin, N.; Michaud, A.; Gendron, D.; Wakim, S.; Blair, E.; Neagu-Plesu, R.; Belletete, M.; Durocher, G.; Tao, Y.; Leclerc, M. *J. Am. Chem. Soc.* **2008**, *130*, 732.
(30) Asawapirom, U.; Guentner, R.; Forster, M.; Farrell, T.; Scherf, U. *Synthesis.* **2002**, 1136.
(31) Kang, S.-M.; Leblebici, Y. *CMOS Digital Integrated Circuits: Analysis and Design*; McGraw-Hill: NewYork, 1996.